VIP MOF Catalysts Very Important Paper

International Edition: DOI: 10.1002/anie.201502094
German Edition: DOI: 10.1002/ange.201502094

Textile/Metal–Organic-Framework Composites as Self-Detoxifying Filters for Chemical-Warfare Agents**

Elena López-Maya, Carmen Montoro, L. Marleny Rodríguez-Albelo, Salvador D. Aznar Cervantes, A. Abel Lozano-Pérez, José Luis Cenís, Elisa Barea, and Jorge A. R. Navarro**

Abstract: *The current technology of air-filtration materials for protection against highly toxic chemicals, that is, chemical-warfare agents, is mainly based on the broad and effective adsorptive properties of hydrophobic activated carbons. However, adsorption does not prevent these materials from behaving as secondary emitters once they are contaminated. Thus, the development of efficient self-cleaning filters is of high interest. Herein, we report how we can take advantage of the improved phosphotriesterase catalytic activity of lithium alkoxide doped zirconium(IV) metal–organic framework (MOF) materials to develop advanced self-detoxifying adsorbents of chemical-warfare agents containing hydrolysable P–F, P–O, and C–Cl bonds. Moreover, we also show that it is possible to integrate these materials onto textiles, thereby combining air-permeation properties of the textiles with the self-detoxifying properties of the MOF material.*

The threat of terrorist attacks with chemical-warfare agents (CWAs) prompts the research on new materials capable of removing toxic chemicals at ambient temperature and humidity.[1,2] In this regard, activated carbons and their modifications with impregnates (metal salts, acids, and amines) are the most widespread materials in air-purification systems. However, the development of self-cleaning materials[3] should be the technology of choice to avoid the contaminated adsorbents behaving as secondary emitters.

Metal–organic frameworks (MOFs) arise as an alternative class of porous materials with a high potential for this application.[1,2] Indeed, the suitability of the established $[Cu_3(btc)_2]$ (btc = benzene-1,3,5-tricarboxylate) system has been studied in the capture and degradation of CWAs,[4–7] however, the results show a poor performance related to its limited stability to hydrolysis.[8] The more robust $[Al_3(OH)F(bdc\_NH_2)_2]$ (NH_2-MIL-101(Al)) and $[AlOH(bdc\_NH_2)]$ (NH_2-MIL-53(Al)) systems, where bdc_NH_2 = 2-aminobenzene-1,4-dicarboxylate, have been assayed for the hydrolysis of the nerve-agent simulant diisopropylfluorophosphate (DIFP) after the covalent attachment of 4-methylaminopyridine nucleophile, to the bdc_NH_2 linkers.[9] In the search for more efficient MOF materials for this application, $[Zr_6O_4(OH)_4(bdc)_6]$ (bdc = benzene-1,4-dicarboxylate) system, named UiO-66 (Figure 1), is receiving attention because of its robustness[10] and the Lewis acidic nature of the Zr^{4+} centers[11] which combined with the basic hydroxide residues gives rise to biomimetic phosphotriesterase activity useful for the hydrolysis of simulants of nerve agents.[12]

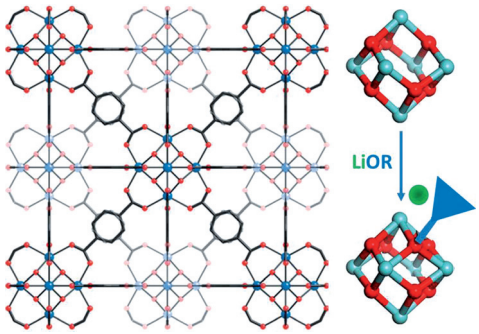

Figure 1. Structure of $[Zr_6O_4(OH)_4(bdc)_6]$ (UiO-66) and schematic representation of the insertion of LiOR in the Zr_6O_6 clusters of the fully activated framework to yield [UiO-66@LiOR] basic catalysts.

Herein, we show different post-synthetic approaches (introduction of acidic and basic sites and/or missing linker defects) to further improve the phosphotriesterase activity of UiO-66 for the capture and hydrolytic degradation of CWA simulants (Figure 1 and Scheme 1). Moreover, we compare the performance of these UiO-66 modified materials with representative "state-of-the-art" porous materials (i.e. activated carbons, hydrophobic MOFs, porous metal oxides) towards the capture and eventual degradation of diisopropylfluorophosphate (DIFP), dimethylmethylphosphonate (DMMP), 2-chloroethylethylsulfide (CEES), and diethylsulfide (DES), as respective models of nerve and vesicant CWAs (Scheme 2). Moreover, we also demonstrate that it is possible to integrate these MOFs on the surface of silk fibroin fibers,

[*] E. López-Maya, Dr. C. Montoro, Dr. L. M. Rodríguez-Albelo, Dr. E. Barea, Prof. J. A. R. Navarro
Departamento de Química Inorgánica
Universidad de Granada
Av. Fuentenueva S/N, 18071 Granada (Spain)
E-mail: ebaream@ugr.es
jarn@ugr.es
Homepage: http://www.ugr.es/local/jarn
Dr. S. D. Aznar Cervantes, Dr. A. A. Lozano-Pérez, Prof. J. L. Cenís
Departamento de Biotecnología, IMIDA, Instituto Murciano de Investigación y Desarrollo Agrario y Alimentario
C/Mayor S/N, 30150 La Alberca, Murcia (Spain)

[**] We thank the Spanish Ministries of Economy (CTQ2011-22787/PPQ, CTQ2014-53486-R) and Defense (COINCIDENTE), MC-IIF (LMRA), Junta de Andalucia (P09-FQM-4981) and ERDF Operative Program of the Region of Murcia 2007–2013 (AALP) for funding.
Supporting information for this article is available on the WWW under http://dx.doi.org/10.1002/anie.201502094.

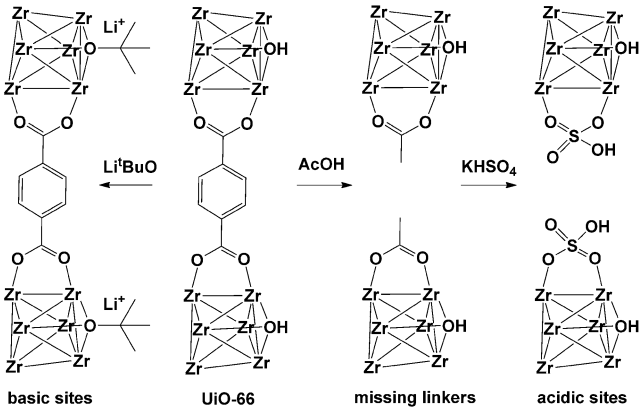

Scheme 1. Routes to improve the catalytic activity of $[Zr_6O_4(OH)_4(bdc)_6]$ (UiO-66) by introduction of missing-linker defects and/or acidic and basic sites.

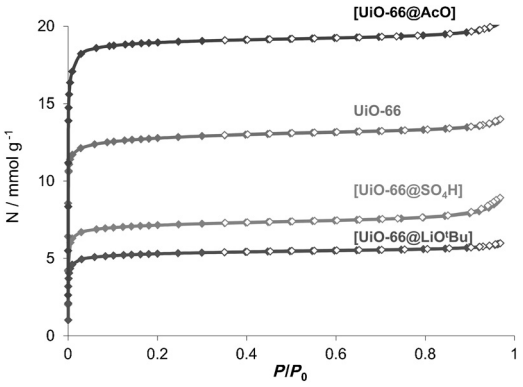

Figure 2. Impact of missing-linker defects and introduction of acidic/basic catalytically active sites on the porosity of UiO-66 framework, as probed by N_2 adsorption at 77 K. Solid symbols denote adsorption, open symbols denote desorption (P/P_O = partial pressure).

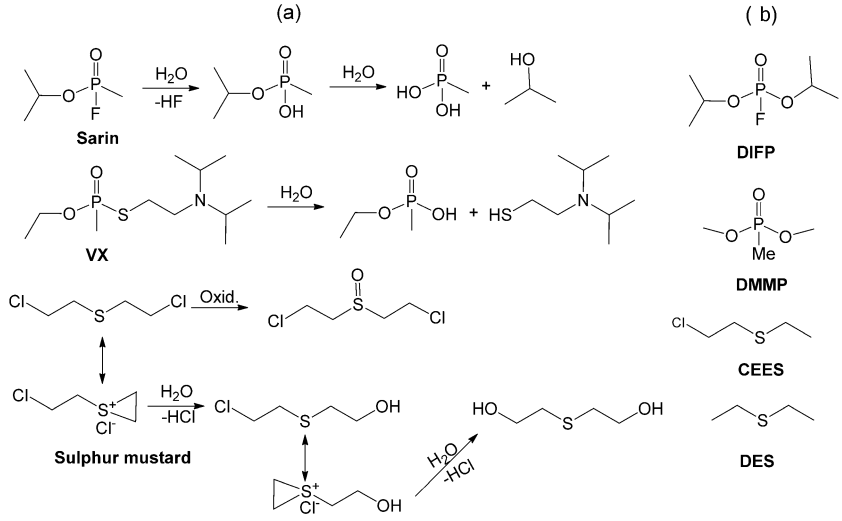

Scheme 2. a) Hydrolytic and oxidative degradation pathways of chemical warfare agents (CWAs): Sarin and VX nerve agents and sulfur mustard vesicant gas; b) CWAs model compounds used in our studies.

giving rise to self-detoxifying protective fabrics, which complement air permeation with adsorption and catalytic degradation of the toxic compounds.

Taking into account all the above, we proceeded to modulate the catalytic activity of both defect-free UiO-66,[10] and missing-linker-defect $[Zr_6O_4(AcO)_6(bdc)_5]$ [UiO-66@AcO][13] by means of the introduction of acidic Brønsted sites in $[Zr_6O_4(AcO)_4(bdc)_5(SO_4H)_2]$ ([UiO-66@SO_4H]) and the insertion of lithium alkoxides in $[Zr_6O_6(bdc)_6(LiO\textit{t}Bu)_{0.3}]$ ([UiO-66@LiO*t*Bu]), $[Zr_6O_8(bdc)_4(LiO\textit{t}Bu)_{0.3}]$ ([UiO-66@AcO_LiO*t*Bu]) and $[Zr_6O_6(bdc)_6(LiOEt)_{0.25}]$ ([UiO-66@LiOEt]).[14] Noteworthy, X-ray powder diffraction studies are indicative that the original **fcu** topology of UiO-66 framework is maintained in the post-synthetically modified materials (see Supporting Information). Likewise, N_2 (77 K) adsorption experiments are indicative that the post-synthetic treatment does not prevent access to the porous network, although, is responsible for either an increase of adsorption capacity in the defect systems or a decrease of capacity after the insertion of HSO_4^- and LiOR functionalities (Figure 2 and Figure S3 in the Supporting Information). Once the modified materials were characterized, we proceeded to evaluate the effect of the post-synthetic functionalization of UiO-66 framework on the eventual catalytic degradation of CWAs analogues DIFP, DMMP, and CEES. In this regard, the hydrolytic pathway is one of the most simple and effective ways of remedying the contamination caused by CWAs molecules (Scheme 2). For this purpose, we have studied the variation of concentration of CWAs models both in the aqueous and adsorbate phases after its exposure to the MOF catalyst at room temperature by GC and ^{31}P-MAS-NMR.

The degradation profiles of DIFP on the essayed materials are summarized in Figure 3 and Figure S6. As it can be appreciated, all the [UiO-66@X] materials are active in the hydrolytic degradation of DIFP whereas hydrophobic MOF materials[8,15] and activated carbon Blücher-101408 which is implemented in "state-of-the-art" Saratoga filtering systems[16] are not (Figure S9 and Table S2). Remarkably, LiO*t*Bu insertion gives rise to the highly active and reusable [UiO-66@LiO*t*Bu] catalyst exhibiting a half-life for P–F bond hydrolysis of 5 min only (turnover frequency (TOF) 0.13 min^{-1}) and full hydrolysis of this bond after 30 min (Figure 3 and Figure S8). The heterogeneity of the catalytic process can also be demonstrated by the loss of catalytic activity after removal of the MOF by filtration (Figure 3b). Analogous results are obtained with [UiO-66@LiOEt] although, the kinetics are slowed, namely, half-life of 30 min (TOF 0.017 min^{-1}) and full conversion after 250 min, which might be attributed to the lower basicity of EtO^- compared to tBuO$^-$. ^{31}P-MAS-NMR studies further confirm the rapid hydrolysis of the P–F bonds (Figure S14). In contrast, both

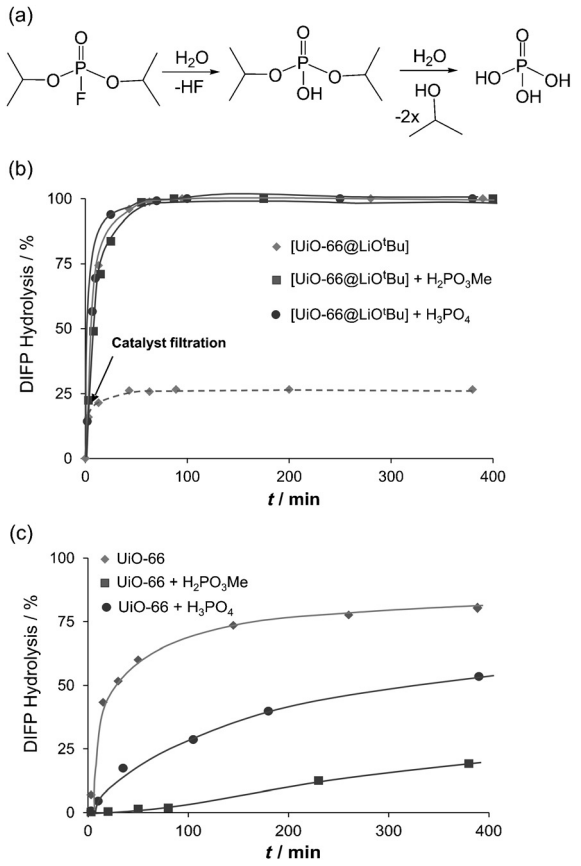

Figure 3. a) Hydrolytic degradation reaction of an aqueous solution of DIFP nerve-gas simulant (0.028 M) catalyzed by b) [UiO-66@LiO*t*Bu] (0.014 mmol) at room temperature (295 K) and c) UiO-66 under the same conditions. The poisoning effect of CWA degradation products on the catalytic activity of UiO-66@X materials, namely, phosphoric acid (0.028 M) and methylphosphonic acid (0.028 M) was also studied. The dotted line in (b) indicates the effect of removal of [UiO-66@LiO*t*Bu] by filtration to demonstrate the heterogeneity of the catalysis.

pristine UiO-66 and defect [UiO-66@AcO] exhibit a three-fold slower kinetics (TOF 0.05 min^{-1}) than [UiO-66@LiO*t*Bu] and their activity is lost after the degradation of approximately 75 % of the DIFP (Figure S6). The loss of activity was indicative of catalyst poisoning, by the degradation products, which was confirmed by the significant decrease in the catalytic activity of UiO-66 after the addition of equimolecular amounts of either methylphosphonic acid (0.014 mmol) or phosphoric acid (0.014 mmol) to the reaction media (Figure 3c). In contrast, the catalytic performance of [UiO-66@LiO*t*Bu] is not affected by methylphosphonic acid or phosphoric acid (Figure 3b). The significant lowering of the catalytic activity of UiO-66 upon the addition of the degradation products (1:6 ratio of degradation product to Zr centers) points to a probable poisoning of the active basic catalytic sites placed at the surface of the UiO-66 nanocrystals. The introduction of acidic HSO_4^- active sites on [UiO-66@SO_4H] is responsible for a further loss of catalytic activity with only 30 % of DIFP degradation being achieved after 6 h (see Figure S6). It should also be noticed that [UiO-66@LiO*t*Bu], clearly outperforms porous ZrO_2 (Figure S6). These results demonstrate the synergistic combination of alkoxide basicity and Lewis acidity of metal centers for improving UiO-66 phosphotriesterase activity.

^{31}P-MAS-NMR spectroscopy studies for [Zn_4O(dimethylcarboxypyrazolate)$_3$][8] are indicative of both a slow adsorption process (half-life of 1 h) and slow degradation of DIFP (half-life of 24 h; Figure S15c). Likewise, hydrophobic MOF materials based on Ni^{II} bis(pyrazolate) systems[15] and activated carbon adsorb DIFP very rapidly from the aqueous phase but once adsorbed DIFP remains intact since the hydrophobic pore structure prevents its hydrolysis, with a concomitant risk of this adsorbent becoming a second emitter (see Figure S9 and Table S2).

To further demonstrate the suitability of the [UiO-66@X] materials towards the degradation of CWAs we have studied their catalytic activity towards the hydrolysis of DMMP (Figure 4) and CEES (Figure 5) which have the characteristic

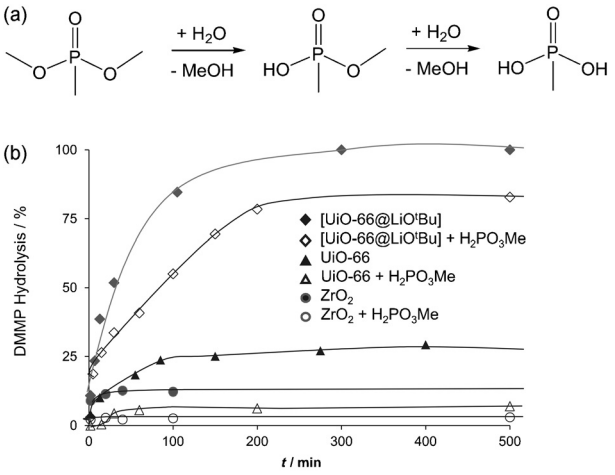

Figure 4. a) Hydrolytic degradation reaction of DMMP nerve-gas simulant; b) degradation profiles of an aqueous solution of DMMP (0.028 M) catalyzed by [UiO-66@LiO*t*Bu], [UiO-66], and porous ZrO_2 at room temperature (295 K). The poisoning effect of methylphosphonic acid (0.028 M) on the catalytic activity of UiO-66@X and ZrO_2 materials is also shown. Solid lines are a guide for the eye.

methylphosphonate and chlorine residues found in nerve agents and vesicant mustard gas, respectively. Once again, [UiO-66@LiO*t*Bu] is the most active material in DMMP degradation, exhibiting a half-life of 25 min (TOF 0.02 min^{-1}) for the first hydrolysis step (Figure 4 and Figure S16). It should also be noted that [UiO-66@LiO*t*Bu] outperforms both NaOH (0.1 M) and LiO*t*Bu (0.1 M) in the homogeneous phase (Figure S10). By contrast, pristine UiO-66 and porous ZrO_2 exhibit a much poorer performance with DMMP with respective degradation values of 30 and 15 % being achieved after 500 min. Finally, while the addition of methylphosphonic acid (0.028 M) to the reaction media gives rise to some poisoning effect of [UiO-66@LiO*t*Bu] catalytic activity (degradation half-life increases to 75 min and TOF decreases to 0.007 min^{-1}), UiO-66 and ZrO_2 become almost inactive (Figure 4).

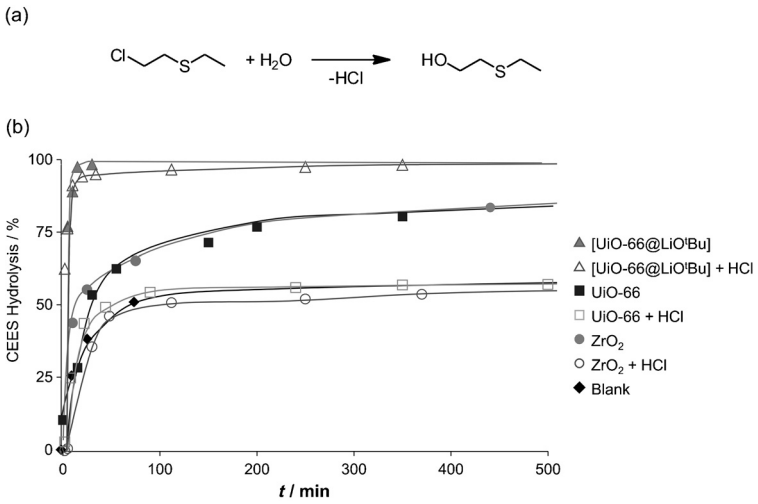

Figure 5. a) Hydrolytic degradation reaction of CEES vesicant gas simulant; b) degradation profiles of an aqueous:ethanolic (1:1) solution of CEES (0.028 M) without catalyst (blank) and in the presence of [UiO-66@LiO*t*Bu], [UiO-66], and porous ZrO_2 at room temperature (295 K). The poisoning effect of HCl (0.028 M) on the catalytic activity of UiO-66@X and ZrO_2 materials is also shown. Solid lines are a guide for the eye.

Similarly, [UiO-66@LiO*t*Bu] is also the most active material in the degradation of CEES exhibiting a half-life of 3 min only (TOF 0.17 min^{-1}) and full conversion to 2-hydroxyethylethylsulfide after 16 min (Figure 5). It should also be noted that [UiO-66@LiO*t*Bu] performance is analogous to NaOH (0.1M) in the homogeneous phase but outperforms LiO*t*Bu (0.1M; Figure S12). Pristine UiO-66 as well as ZrO_2 exhibit a much poorer performance with only partial degradation values of CEES, namely 80% being achieved after 500 min, indicative of catalyst poisoning (Figure 5). Indeed, while the addition of hydrochloric acid (0.028 M) does not affect significantly the catalytic activity of [UiO-66@LiO*t*Bu] (degradation half-life increases to 3.4 min) in the case of UiO-66 and porous ZrO_2 the catalytic activity is lost and their behavior becomes analogous to the control (Figure 5).

Taking all the above results into consideration, we thought of the possibility of integrating these materials into protective fabrics to combine the self-detoxifying properties of the catalysts with the air permeation of the textiles. With this purpose, we chose silk fibroin fabrics as a proof-of-concept textile owing to its biocompatibility, resistance, and lightness. The procedure of MOF deposition onto the fibers consisted of spraying a methanolic sonicated suspension of the desired MOF onto electrospun silk fibroin which, after appropriate curing, gave rise to hybrid silk@MOF composites with to 1:1 silk to MOF ratios. The images of scanning electron microscopy show the successful deposition of both UiO-66 and [UiO-66@LiO*t*Bu] MOF nanocrystals (ca. 200 nm) on silk fibers (ca. 1 μm wide) (Figure 6a and Figure S17). Moreover, X-ray powder diffraction (XRPD) and N_2 adsorption measurements are diagnostic that both the MOF crystallinity and the porosity of the MOF materials are maintained while air permeability of the textile fabric is preserved (Supporting Information). Note that the silk@[UiO-66@LiO*t*Bu] composite textile exhibits the best performance towards the degradation of the CWA analogues with respective degradation half-lives of 20 min (TOF 0.025 min^{-1}), 50 min (TOF 0.01 min^{-1}), and 8 min (TOF 0.06 min^{-1}) for DIFP, DMMP, and CEES (Figure 6b–d). Moreover, the removal of the silk@-MOF composites stops the reaction, an indication

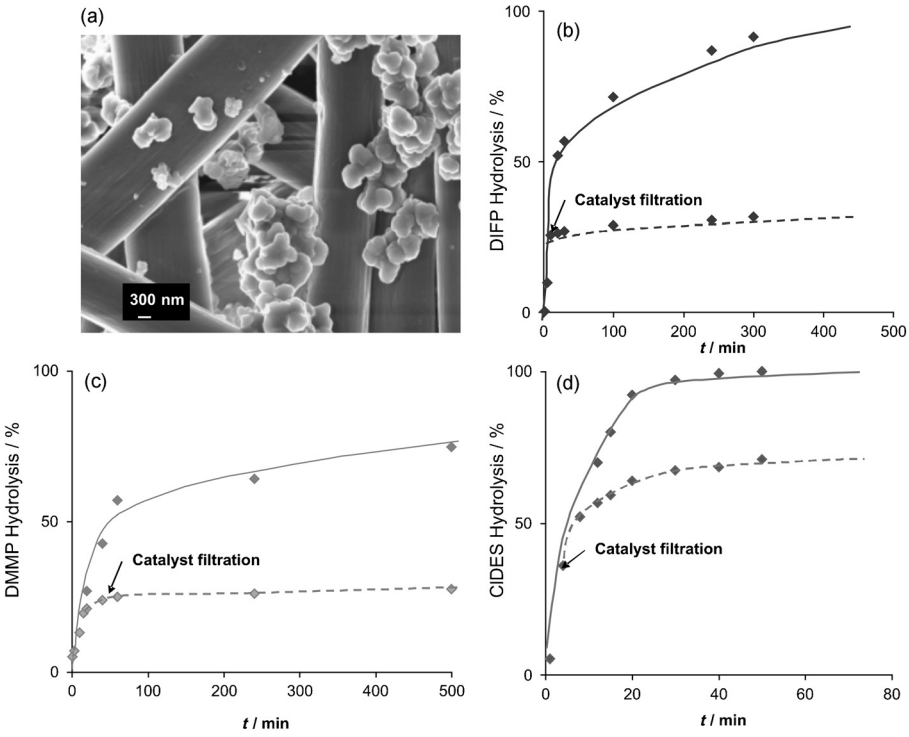

Figure 6. a) VP-SEM (VP = variable pressure) images of silk@[UiO-66@LiO*t*Bu] composite. Hydrolytic degradation profiles of b) DIFP, c) DMMP, and d) CEES, all catalyzed by silk@[UiO-66@LiO*t*Bu] composite at room temperature. The dotted lines indicate the effect of removing the [UiO-66@LiO*t*Bu] by filtration to demonstrate the heterogeneity of the catalytic process.

of the heterogeneous nature of the catalysis and that lack of MOF leaching from the fabric.

It can be concluded that the insertion of lithium alkoxides in the zirconium oxide clusters gives rise to a boosting of the phosphotriesterase catalytic activity for the hydrolysis of P–F,

P–O, and C–Cl bonds typically found in CWAs. Furthermore, these features can also be integrated into self-detoxifying protective fabrics which combine air permeation and self-detoxifying properties. Computational work is in progress to fully understand the behavior of the UiO-66 modified catalysts.[17]

Keywords: heterogeneous catalysis · hydrolysis · metal–organic frameworks · nerve agents · silk fibroin

How to cite: *Angew. Chem. Int. Ed.* **2015**, *54*, 6790–6794
Angew. Chem. **2015**, *127*, 6894–6898

[1] J. B. DeCoste, G. W. Peterson, *Chem. Rev.* **2014**, *114*, 5695–5727.
[2] E. Barea, C. Montoro, J. A. R. Navarro, *Chem. Soc. Rev.* **2014**, *43*, 5419–5430.
[3] *Self-Cleaning Materials and Surfaces: A Nanotechnology Approach* (Eds.: W. A. Daoud), Wiley, Chichester, **2013**.
[4] G. W. Peterson, G. W. Wagner, *J. Porous Mater.* **2014**, *21*, 121–126.
[5] A. Roy, A. K. Srivastava, B. Singh, T. H. Mahato, D. Shah, A. K. Halve, *Microporous Mesoporous Mater.* **2012**, *162*, 207–212.
[6] A. Roy, A. K. Srivastava, B. Singh, D. Shah, T. H. Mahato, P. K. Gutch, A. K. Halve, *J. Porous Mater.* **2013**, *20*, 1103–1109.
[7] A. Roy, A. K. Srivastava, B. Singh, D. Shah, T. H. Mahato, A. Srivastava, *Dalton Trans.* **2012**, *41*, 12346–12348.
[8] C. Montoro, F. Linares, E. Quartapelle Procopio, I. Senkovska, S. Kaskel, S. Galli, N. Masciocchi, E. Barea, J. A. R. Navarro, *J. Am. Chem. Soc.* **2011**, *133*, 11888–11891.
[9] L. Bromberg, Y. Klichko, E. P. Chang, S. Speakman, C. M. Straut, E. Wilusz, T. A. Hatton, *ACS Appl. Mater. Interfaces* **2012**, *4*, 4595–4602.
[10] J. H. Cavka, S. Jakobsen, U. Olsbye, N. Guillou, C. Lamberti, S. Bordiga, K. P. Lillerud, *J. Am. Chem. Soc.* **2008**, *130*, 13850–13851.
[11] L. Valenzano, B. Civalleri, S. Chavan, S. Bordiga, M. H. Nilsen, S. Jakobsen, K. P. Lillerud, C. Lamberti, *Chem. Mater.* **2011**, *23*, 1700–1718.
[12] M. J. Katz, J. E. Mondloch, R. K. Totten, J. K. Park, S. T. Nguyen, O. K. Farha, J. T. Hupp, *Angew. Chem. Int. Ed.* **2014**, *53*, 497–501; *Angew. Chem.* **2014**, *126*, 507–511.
[13] H. Wu, Y. S. Chua, V. Krungleviciute, M. Tyagi, P. Chen, T. Yildirim, W. Zhou, *J. Am. Chem. Soc.* **2013**, *135*, 10525–10532.
[14] R. Ameloot, M. Aubrey, B. M. Wiers, A. P. Gómora-Figueroa, S. N. Patel, N. P. Balsara, J. R. Long, *Chem. Eur. J.* **2013**, *19*, 5533–5536.
[15] N. M. Padial, E. Quartapelle Procopio, C. Montoro, E. López, J. E. Oltra, V. Colombo, A. Maspero, N. Masciocchi, S. Galli, I. Senkovska, S. Kaskel, E. Barea, J. A. R. Navarro, *Angew. Chem. Int. Ed.* **2013**, *52*, 8290–8294; *Angew. Chem.* **2013**, *125*, 8448–8452.
[16] http://www.bluecher.com.
[17] While this article was in press we learned of two related studies: S. Y. Moon, Y. Liu, J. T. Hupp, O. K. Farha *Angew. Chem. Int. Ed.* **2015**, *54*, 6795–6799; *Angew. Chem.* **2015**, *127*, 6899–6903; J. E. Mondloch, M. J. Katz, W. C. Isley III, P. Ghosh, P. Liao, W. Bury, G. W. Wagner, M. G. Hall, J. B. DeCoste, G. W. Peterson, R. Q. Snurr, C. J. Cramer, J. T. Hupp, O. K. Farha, *Nature Mater.* **2015**, DOI: 10.1038/NMAT4238.

Received: March 7, 2015
Published online: May 7, 2015

